photonics

MDPI

Article

Tailoring the Direct Current Modulation Response of Electrically Pumped Semiconductor Nano-Laser Arrays

Yuanlong Fan [1,*], Siyi An [1], K. Alan Shore [2,*] and Xiaopeng Shao [1]

[1] Hangzhou Institute of Technology, Xidian University, Hangzhou 311200, China; 22191214999@stu.xidian.edu.cn (S.A.); xpshao@xidian.edu.cn (X.S.)
[2] School of Computer Science and Electronic Engineering, Bangor University, Bangor LL57 1UT, UK
* Correspondence: fanyuanlong@xidian.edu.cn (Y.F.); k.a.shore@bangor.ac.uk (K.A.S.)

Abstract: Semiconductor nano-lasers have been a topic of interest from the perspective of advancing the capabilities of photonic integration. Nano-lasers are perceived as the means to achieve improved functionality in photonic integrated circuits. The properties and performance of nano-lasers have been examined by means of simulations and laboratory measurements. Nano-lasers lend themselves to integration to form dense arrays in both one and two dimensions. In a recent work, a theoretical treatment was presented for the dynamic behaviour of stand-alone electrically pumped nano-laser arrays. In this work, the response of nano-laser arrays to direct current modulation is examined. As in previous works, attention is given to two prototype array geometries: a linear three-element linear array and an equilateral triangular array. Large one-dimensional arrays can be built by repeating this elementary linear array. Two-dimensional photonic integrated circuits can incorporate the triangular arrays studied here. Such prototypical configurations offer opportunities to tailor the modulation response of the nano-laser arrays. The principal factors which provide that capability are the coupling strengths between lasers in the arrays and the direct modulation parameters. The former are fixed at the design and manufacture stage of the array whilst the latter can be chosen. In addition, the enhancement of the spontaneous emission rate via the so-called Purcell effect in nano-lasers offers a device-specific means for accessing a range of modulation responses. Two-dimensional portraits of the regimes of differing modulation responses offer a convenient means for determining the dynamics that may be accessed by varying the laser drive current. It is shown by these means that a rich variety of modulation responses can be accessed in both linear and triangular arrays.

Keywords: semiconductor nano-lasers; laser dynamics; laser arrays

Citation: Fan, Y.; An, S.; Shore, K.A.; Shao, X. Tailoring the Direct Current Modulation Response of Electrically Pumped Semiconductor Nano-Laser Arrays. *Photonics* **2023**, *10*, 1373. https://doi.org/10.3390/photonics10121373

Received: 31 October 2023
Revised: 13 December 2023
Accepted: 13 December 2023
Published: 14 December 2023

1. Introduction

Prospects for semiconductor nano-lasers have been explored over a significant period of time [1–4]. The practical realization of nano-lasers is particularly significant in the case of optical pumping with nano-lasers, having been achieved with a number of active media [5–8]. Contrariwise, the demonstration of electrically pumped semiconductor nano-lasers has been found to be technically challenging and, in consequence, the number of reports on their successful demonstration has been small [9–14]. Nevertheless, considerable efforts have been made to simulate the dynamic behaviour of electrically driven nano-lasers [15–17]. Mention may be made of extensive works which have addressed the response of electrically pumped nano-lasers to external perturbations including their direct current modulation behaviour [18], when they are subject to an external optical injection [19], and when they are affected by both regular [20] and phase conjugate [21] optical feedback. In general, such works have considered the response of isolated semiconductor nano-lasers. But some effort has also been directed towards determining the dynamic behaviour of mutually coupled nano-lasers [22]. In the context of such extensive simulations, it is hoped that the implementation of electrically pumped semiconductor nano-lasers will

facilitate opportunities to undertake experimental measurements of the rich dynamics of semiconductor nano-lasers.

Semiconductor nano-lasers naturally lend themselves to the configuration of one and two-dimensional arrays. A recent valuable survey [23] showed the potential practical applications of nano-laser arrays and included a pioneering analysis of the dynamics of two-element arrays. In that case, it was also possible to make reference to seminal experimental results obtained with optically pumped nano-laser arrays. In such arrays, coupling between array elements can be expected to significantly impact both the static and dynamic behaviours of the nano-laser arrays. A particular aspect of the static behaviour is the nature of the near- and far-field emissions of the array. In [23], attention is, e.g., given to a super-mode formation in two-element nano-laser arrays. In contrast, in a recent work [24], the dynamic behaviour of stand-alone electrically pumped nano-laser arrays was explored in some detail. As is well appreciated, the evanescent coupling strength between elements of such an array is determined by the geometry of the lasers and the spacing between them. There are no extant examples of electrically pumped nano-laser arrays from which we may derive information of coupling strength; hence, we treated the coupling strength as a parameter. The present work seeks to advance that study by taking into account a specific external perturbation viz direct current modulation. For the purpose of this study, we assume that an appropriate electrical isolation is incorporated between the elements of the nano-laser array to eliminate electrical cross-talk so that we may independently modulate the array elements. It is noted here that other external perturbations may be anticipated to yield novel dynamic behaviours—as has been found in studies of single nano-lasers.

As in our previous work [24], attention is given here to three-element nano-laser arrays: a linear three-element array and a triangular array. These configurations are seen as elementary elements of large one- and two-dimensional nano-laser arrays, respectively. It was observed [24] that the scope for investigating even such simple assemblies is rather large, and, hence, no claim is made that the present study is exhaustive. Indeed, specific indicators are given of directions for further exploration. Ipso facto, a comprehensive categorization of the direct modulation response is challenging. As such, we aim to delineate a variety of experimentally accessible responses to direct current modulation.

In many respects, nano-lasers and, hence, nano-laser arrays are similar to regular semiconductor lasers; thus, there is a physical phenomenon which can be accessed in nano-lasers but is unavailable in other semiconductor lasers: the enhancement of spontaneous emission via the Purcell effect. This enhancement is characterized in simulations using the Purcell enhancement factor. Accordingly, considerable attention is given here to delineating the impact of the Purcell factor on the modulation response of nano-laser arrays. The model utilised in the present simulations is detailed in the next section. Section 3 comprises simulation results for the direct current modulation response of both linear three-element arrays and triangular arrays. Section 3 also contains some indicators of additional opportunities for beneficially exploring the modulation response of these prototype arrays. Section 4 offers a brief conclusion and further pointers to how the present simulations may be extended.

2. Model

The target structures for the simulations of 3-element nano-laser linear and triangular arrays subject to direct current modulation are displayed schematically in Figure 1. The modulation properties of the laterally coupled nano-lasers were modelled using a modified form of coupled rate equations [25,26] with the Purcell-enhanced spontaneous emission factor F and spontaneous emission factor β included, as introduced in [27]. The direct current modulation response of these arrays is described by the following model.

$$\frac{dS_j(t)}{dt} = \frac{\Gamma F \beta N_j(t)}{\tau_n} + \Gamma g_n[N_j(t) - N_0]S_j(t) - \frac{S_j(t)}{\tau_p} - \sum_{\substack{m=1 \\ m \neq j}}^{M} 2k_{jm}S_m(t)\sin[\phi_m(t) - \phi_j(t)] \quad (1)$$

$$\frac{d\phi_j(t)}{dt} = \frac{\alpha}{2}\left\{\Gamma g_n[N_j(t) - N_0] - \frac{1}{\tau_p}\right\} + \sum_{\substack{m=1 \\ m \neq j}}^{M} \left\{\Delta\omega_{jm} + k_{jm}\frac{S_m(t)}{S_j(t)}\cos[\phi_m(t) - \phi_j(t)]\right\} \quad (2)$$

$$\frac{dN_j(t)}{dt} = \frac{I_j(t)}{eV_a} - \frac{N_j(t)}{\tau_n}[F\beta + (1-\beta)] - g_n[N_j(t) - N_0]S_j(t) \quad (3)$$

where the subscripts 'j' and 'm' represent the jth and mth laser, respectively. M is the number of lasers in the array. t is the time. $S(t)$ is the photon density, $\phi(t)$ is the optical phase, $N(t)$ is the carrier density, and $I(t)$ is the injected modulation current. $I(t) = I_0[1 + m\cos(2\pi f_m t)]$, where I_0 is the bias current, m is the modulation index, and f_m is the modulation frequency. Γ is the confinement factor, τ_n is the carrier lifetime, g_n is the differential gain, N_0 is the transparency carrier density, τ_p is the photon lifetime, k is the coupling rate between the two lasers, α is the linewidth enhancement factor, $\Delta\omega$ is the frequency detuning between the two lasers, e is the elementary charge, and V_a is the volume of the active region.

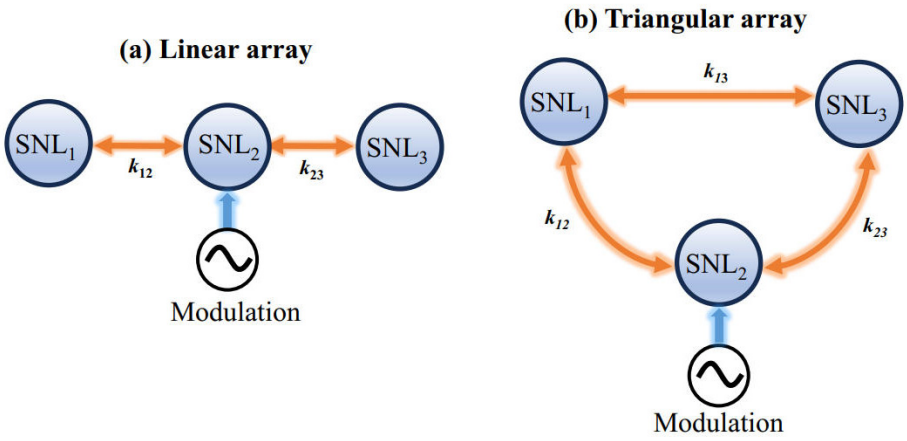

Figure 1. Schematic diagrams of 3-element semiconductor nano-laser (SNL) arrays with modulation. k_{12}, k_{13}, and k_{23} represent the coupling rate between each pair of lasers. (**a**) Linear array; (**b**) triangular array.

Equations (1)–(3) were solved numerically using a fourth order Runge–Kutta integration method. The 3-element arrays, i.e., $M = 3$, were simulated, which required the solution of 9 coupled rate equations. In the simulations, a temporal resolution of $\Delta t = 0.1$ *ps* was selected, and the duration of the time series was set to 1 µs. The dynamics of the nano-lasers were analysed using the device parameters given in Table 1, which are mainly from [12,28].

Table 1. Nano-laser device parameters.

Symbol	Physical Meaning	Value
β	Spontaneous emission factor	0.05
Γ	Confinement factor	0.65
τ_n	Carrier lifetime	2.00×10^{-9} s
g_n	Differential gain	1.65×10^{-12} m^3/s
N_0	Carrier density at transparency	1.10×10^{24} m^{-3}

Table 1. *Cont.*

Symbol	Physical Meaning	Value
τ_p	Photon lifetime	0.36×10^{-12} s
k	Coupling rate	variable
α	Linewidth enhancement factor	variable
$\Delta\omega$	Frequency detuning	0 GHz
e	Elementary charge	1.60×10^{-19} C
V_a	Volume of the active region	3.96×10^{-19} m^3

3. Results

The aim of this study was to investigate the dynamic behaviour of laterally coupled nano-laser arrays in which one of the lasers is subject to direct current modulation.

3.1. Linear Array

A feature of the system which can be easily changed experimentally is the laser modulation index. It is of interest, therefore, to characterize the dynamics of the system as a function of modulation index. The results are shown in Figure 2 as a 2D map which was generated for coupling rates in the range of $0 < k_{12}\tau_p < 1.8 \times 10^{-3}$ and modulation index in the range of $0.2 < m < 0.5$ to show the dynamic behaviours of nano-lasers. All lasers were biased at twice the threshold, $I_0 = 2I$th, where Ith is the threshold current. In Figure 2, six different representative dynamics were chosen as points A–F. The time series of these dynamics are shown in Figure 3. An important issue is the extent to which the modulated behaviour of one laser affects that of the other. Such an interaction may, in general, be termed cross-talk. From Figure 2, a wide range of zero-cross-talk regions (stable) exists in nano-lasers 1 and 3. In this region, the nano-lasers act independently of each other, and the response of the lasers is simply at the modulation frequency of the individual laser (or possibly at a harmonic of that frequency) [29]. The facility to individually address a given nano-laser without affecting the behaviour of the other laterally coupled nano-lasers should find ready applications in dense photonic integrated circuits.

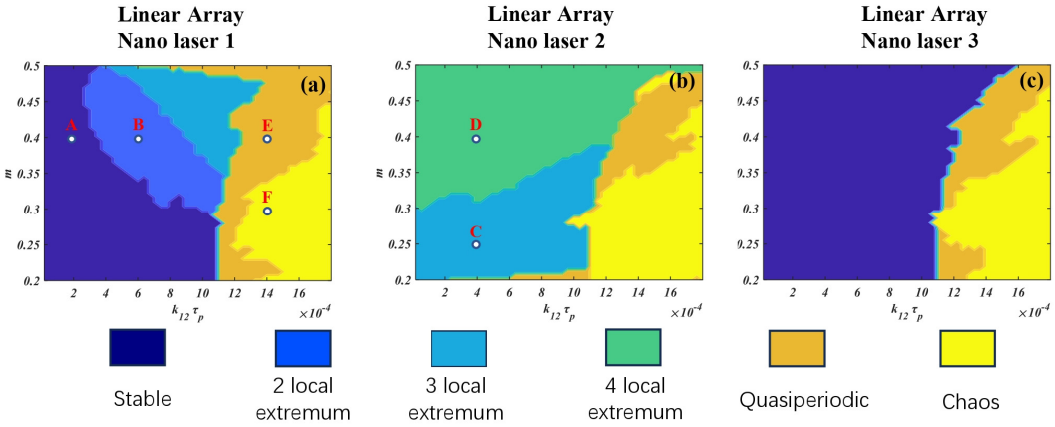

Figure 2. Two-dimensional maps of dynamics of 3-element linear array nano-lasers 1–3 with modulation when $F = 2$, $\alpha = 2$, $f_m = 10$ GHz and $k_{23}\tau_p = 1.8 \times 10^{-4}$. (**a**) Nano-laser 1; (**b**) nano-laser 2; (**c**) nano-laser 3.

In Figure 4, the effect of modulation frequency, F, and α is presented. With the increase in f_m (shown as the first and second rows of Figure 4), the zero-cross-talk region in nano-lasers 1 and 3 shrinks significantly. However, nano-laser 2′s dynamics uniformly display two local extremums, a property which is preserved. With the increase in F, as shown in the third row of Figure 4, the zero-cross-talk region in nano-lasers 1 and 3 expands. Finally, the effect of α is shown in the fourth row of Figure 4, from which the increase in α can destabilize the lasers so that a large region of chaos appears.

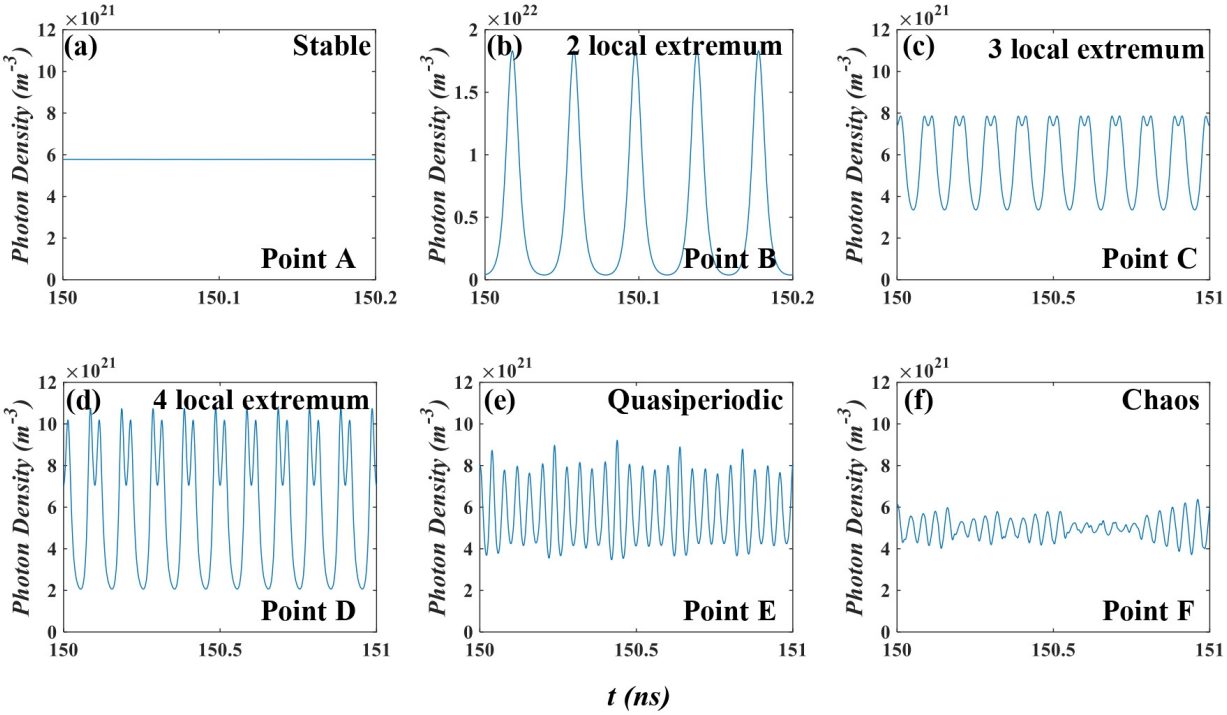

Figure 3. Time series of nano-lasers' dynamics corresponding to points A–F in Figure 2.

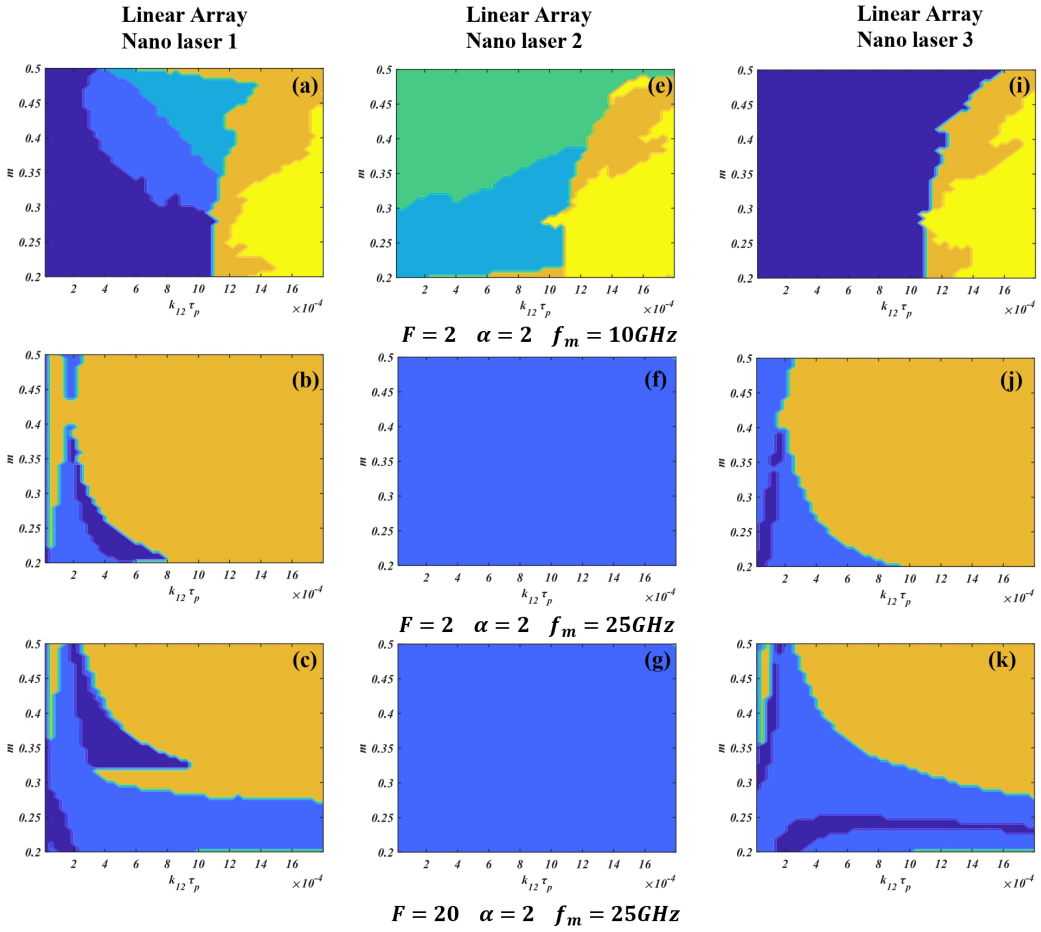

Figure 4. *Cont.*

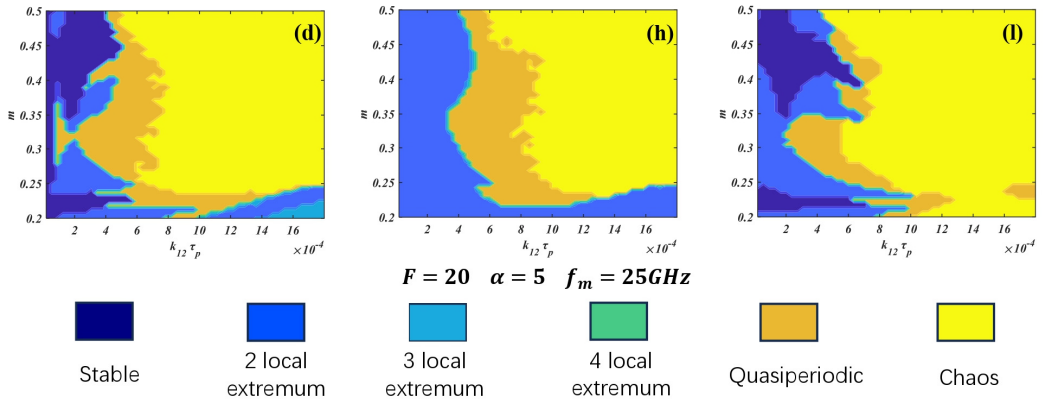

Figure 4. Two-dimensional maps of dynamics of 3-element linear-array nano-lasers 1–3 with modulation for different F, different α, and different f_m values when $k_{23}\tau_p = 1.8 \times 10^{-4}$ and $I_0 = 2\,I$th.

Figure 5 shows the effect of coupling rate between nano-lasers 2 and 3, i.e., k_{23} on the dynamic behaviours. For a relatively small k_{23}, i.e., $k_{23}\tau_p = 1.8 \times 10^{-5}$ and 3.6×10^{-5}, the modulation of nano-laser 2 does not affect nano-laser 3 (see Figure 5i,j). However, with a further increase in k_{23} to 1.8×10^{-3}, the zero-cross-talk region disappears in nano-laser 3 and is replaced by more complex dynamics.

In an experimental context, a convenient parameter for variation is the laser bias current. As shown in Figure 6, results obtained with several different values of the bias current are present. It is seen that the dynamic domains in all lasers change markedly with the increase in bias current. For nano-laser 1 (Figure 6a–c), the increase in the bias current first increases and then decreases the extent of the stable behaviour. Chaotic behaviour is expunged at higher bias, currents but quasi-periodic dynamics persist. In nano-laser 2 (Figure 6d–f), a lower bias current provides access to domains of regular behaviour, quasi-periodic dynamics, and chaos. As the bias current is increased, chaos and quasi-periodic dynamics are removed, and the predominant feature is the increase in areas of regular dynamics. Regions of stability in nano-laser 3 are eliminated as the bias current is increased (Figure 6g–i). Significant regions of quasi-periodic dynamics appear, sometimes interlaced with chaotic behaviour (Figure 6i).

Another feature of the system which can be easily changed experimentally is the frequency detuning between each pair of lasers. Figure 7 displays the dynamics of the system as a function of frequency detuning, i.e., ω_{12} and ω_{23}. The effect of coupling strength on such a 2D map is also explored in Figure 7. It is noted that such variations of the coupling strength must be considered at the design and fabrication stages and are not parameters which are available for variation within laboratory experiments. Such variations do, however, yield the most dramatic changes in the response of the array elements. Nano-laser 1 (Figure 7a–c) is stable for lower coupling strengths and then exhibits the full gamut of dynamic behaviour for the largest value of the coupling coefficient. Nano-laser 2 (Figure 7d–f) transitions through regimes of regular motion to an amalgam of regular and quasi-periodic behaviour. Nano-laser 3 (Figure 7g–i) is strikingly stable for lower values of the coupling coefficient and then exhibits bands of regular and irregular behaviours. At the higher coupling values, the portraits of the dynamics of all the nano-lasers display diagonal lines of regular dynamics. In these calculations, all other parameters were fixed, so it may be expected that other compositions of dynamics may be accessed with an appropriate choice of parameters, including the bias current.

In the next section, attention is given to the dynamics of nano-lasers with modulation in a triangular configuration as a prototype structure for creating two-dimensional nano-laser arrays. But it is first noted that parallel arrangements of linear arrays may also be used to create two-dimensional arrays. There is considerable scope for the calculations of their behaviour.

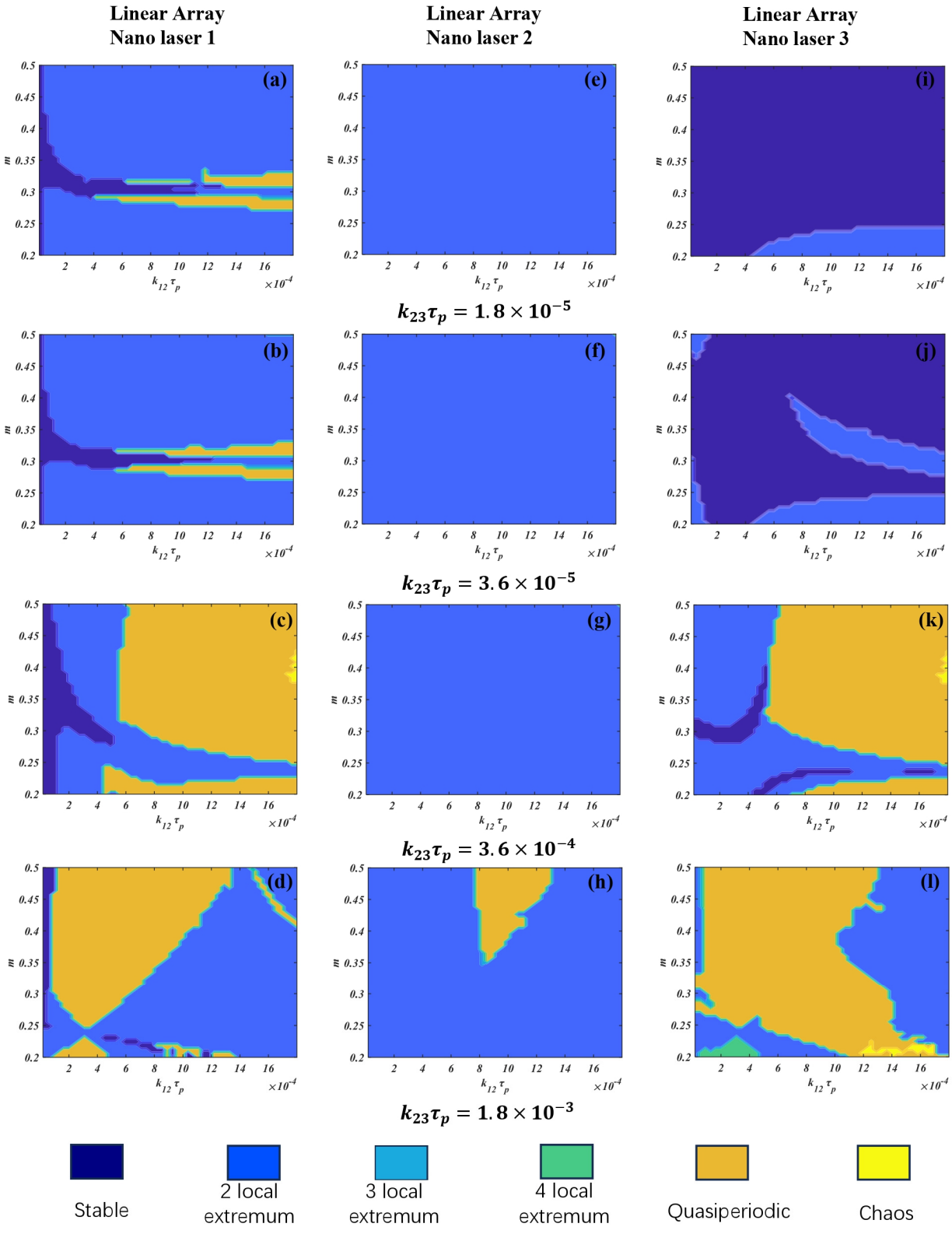

Figure 5. Two-dimensional maps of dynamics of 3-element linear-array nano-lasers 1–3 with modulation for different $k_{23}\tau_p$ values when $F = 20$, $\alpha = 2$, $f_m = 25$ GHz, and $I_0 = 2$ *I*th.

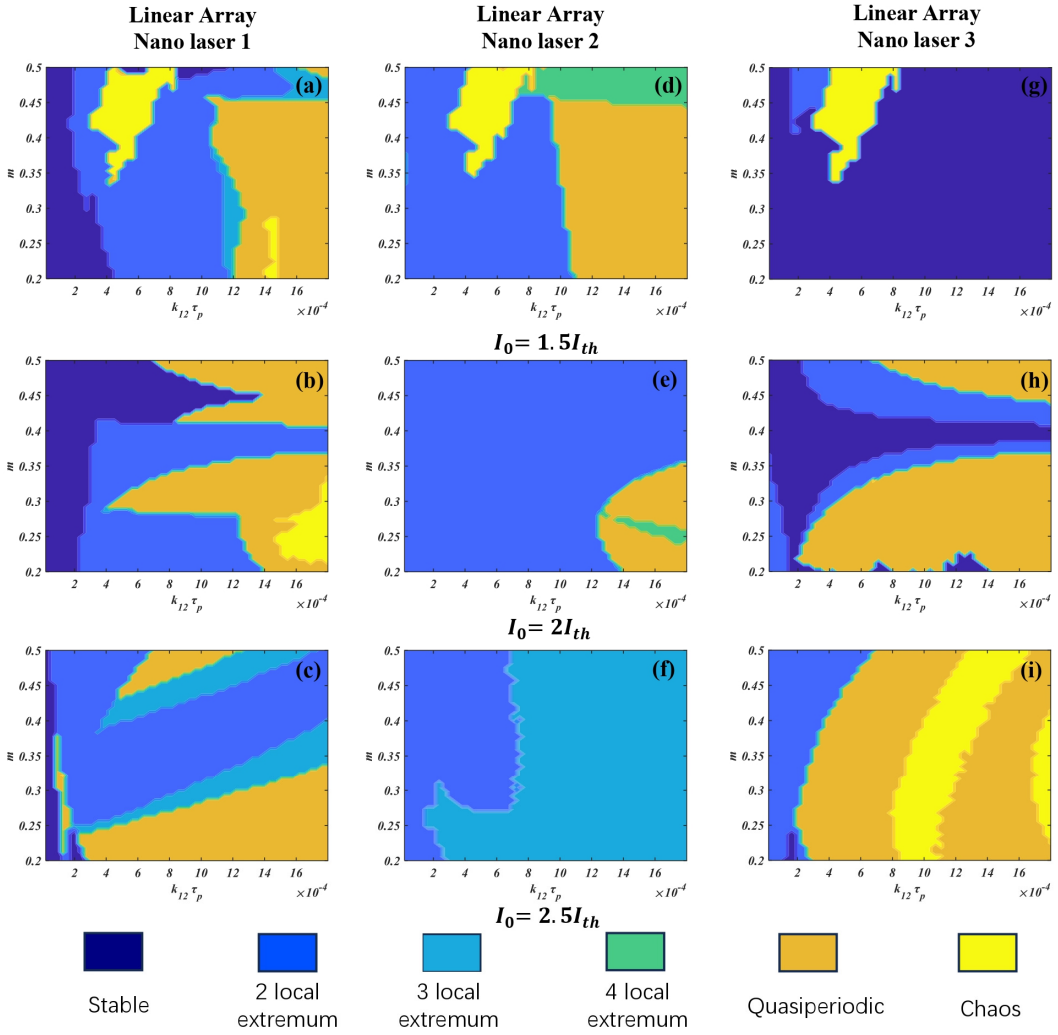

Figure 6. Two-dimensional maps of dynamics of 3-element linear-array nano-lasers 1–3 with modulation for different I_0 values when $F = 40$, $\alpha = 2$, $f_m = 25$ GHz, and $k_{23}\tau_p = 1.8 \times 10^{-4}$.

3.2. Triangular Array

The foregoing results have shown that the variation of laser drive current and inter-element coupling strength gives rise to a great variety of dynamics; as such, the same parameters are utilised in studying the direct current modulation response of triangular nano-laser arrays. As indicated in Figure 1, mainly for reasons of simplicity, modulation is applied only to nano-laser 2. An exploration of the response to multiple modulations is clearly possible but not addressed here. The results demonstrate that several species of modulation response can be easily accessed. The same qualitative trends appear as in the case of the linear array, albeit that the detailed features of the dynamics of individual nano-lasers vary considerably. As with the case of linear arrays, it is observed that some behaviours appear within relatively narrow parameter ranges and, hence, may not necessarily be sufficiently robust to be observed experimentally. Nevertheless, there is a sufficiently rich variety of dynamics which should be capable of exploitation.

Figure 8 delineates the dynamics displayed by each element of the triangular array as we vary some combinations of the Purcell factor, F, the linewidth enhancement factor, α, and the modulation frequency, f_m. The coupling strength between nano-lasers 1 and 3 and 2 and 3 are set as $k_{13}\tau_p = k_{23}\tau_p = 1.8 \times 10^{-4}$. For lower values of all these parameters ($F = 2$; $\alpha = 2$; $f_m = 10$ GHz), each laser exhibits several forms of regular behaviour and enters regimes of chaotic dynamics as the modulation index and/or coupling strength is changed. Both nano-laser 1 and nano-laser 3 have extensive regions of zero-cross-talk (stable) behaviours. With

the increase in the modulation frequency to 25 GHz but the other parameters remaining unchanged, nano-laser 2 resides in a state of two local extrema whilst nano-lasers 1 and 3 predominantly display quasi-periodic and periodic dynamics. The regions of zero-cross-talk are significantly atrophied. Regimes of chaos are also small. Increasing the Purcell factor by an order of magnitude at the higher modulation frequency does not markedly change the range of behaviours obtained. However, a significant change is manifest when the linewidth enhancement factor is increased from 2 to 5, respectively. In these cases, all the lasers exhibit chaos over a wide area in the modulation index—coupling parameter space as well as significant regimes of quasi-periodic and regular dynamic behaviours.

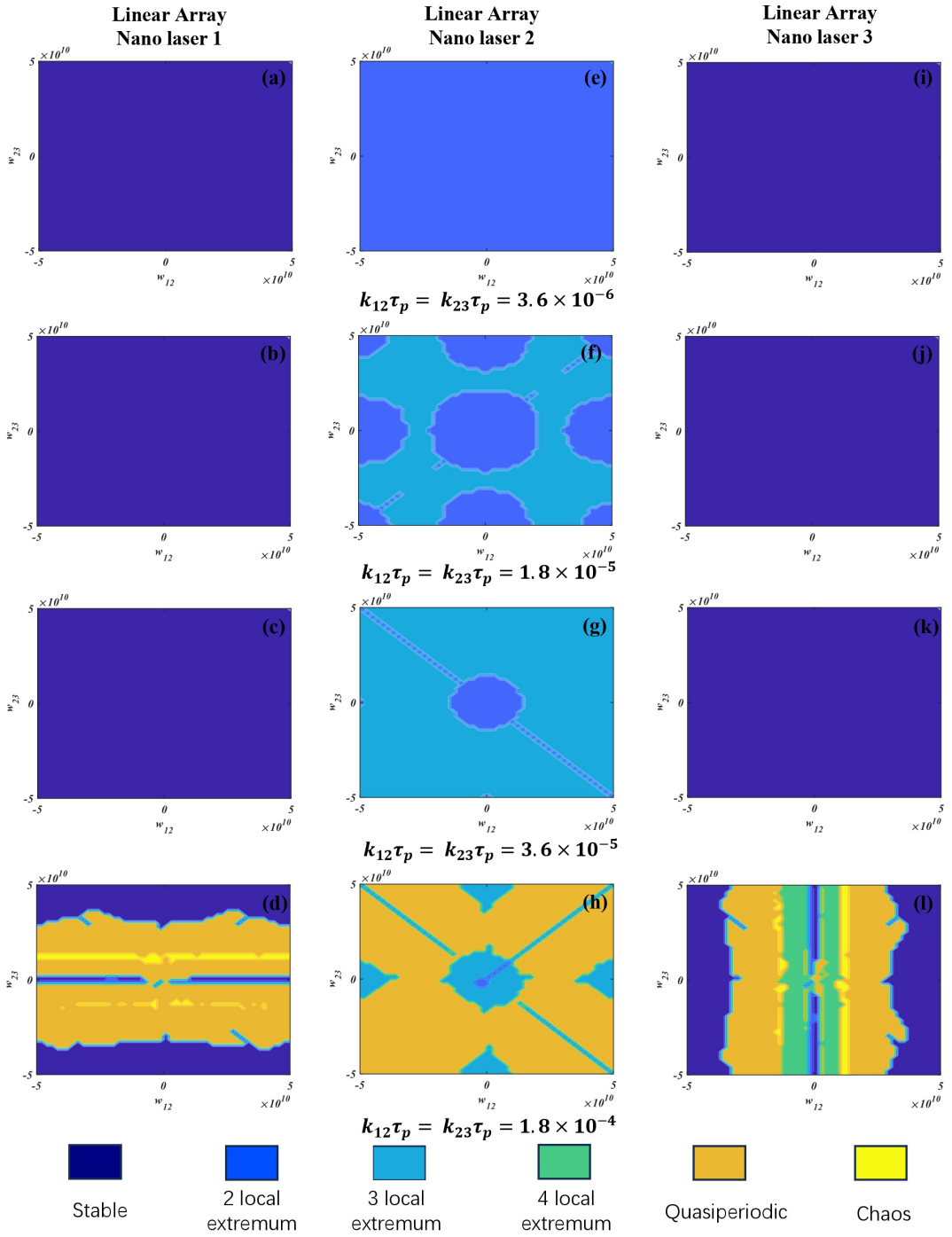

Figure 7. Two-dimensional maps of dynamics of 3-element linear-array nano-lasers 1–3 with modulation for different coupling strengths when $F = 20$, $\alpha = 2$, $f_m = 25$ GHz, and $I_0 = 2$ *I*th.

In Figure 9 attention is focussed on the role of the coupling strength between the lasers in determining the behaviours which may be expected from modulated nano-laser arrays. Here, the Purcell factor, F, the linewidth enhancement factor, α, and the modulation frequency, f_m, are held fixed: $F = 20$, $\alpha = 2$, and $f_m = 25$ GHz. The effect of coupling strength between nano-lasers 2 and 3 is considered whilst the coupling strength between nano-lasers 1 and 3 is kept constant as $k_{13}\tau_p = 1.8 \times 10^{-4}$. The difference in coupling strengths between each laser causes the asymmetry of dynamics in nano-lasers 1 and 3, as shown in Figures 5 and 9. As the coupling strength is increased, the response of nano-laser 2 is largely unchanged, albeit showing some quasi-periodic behaviour for the strongest coupling strength considered.

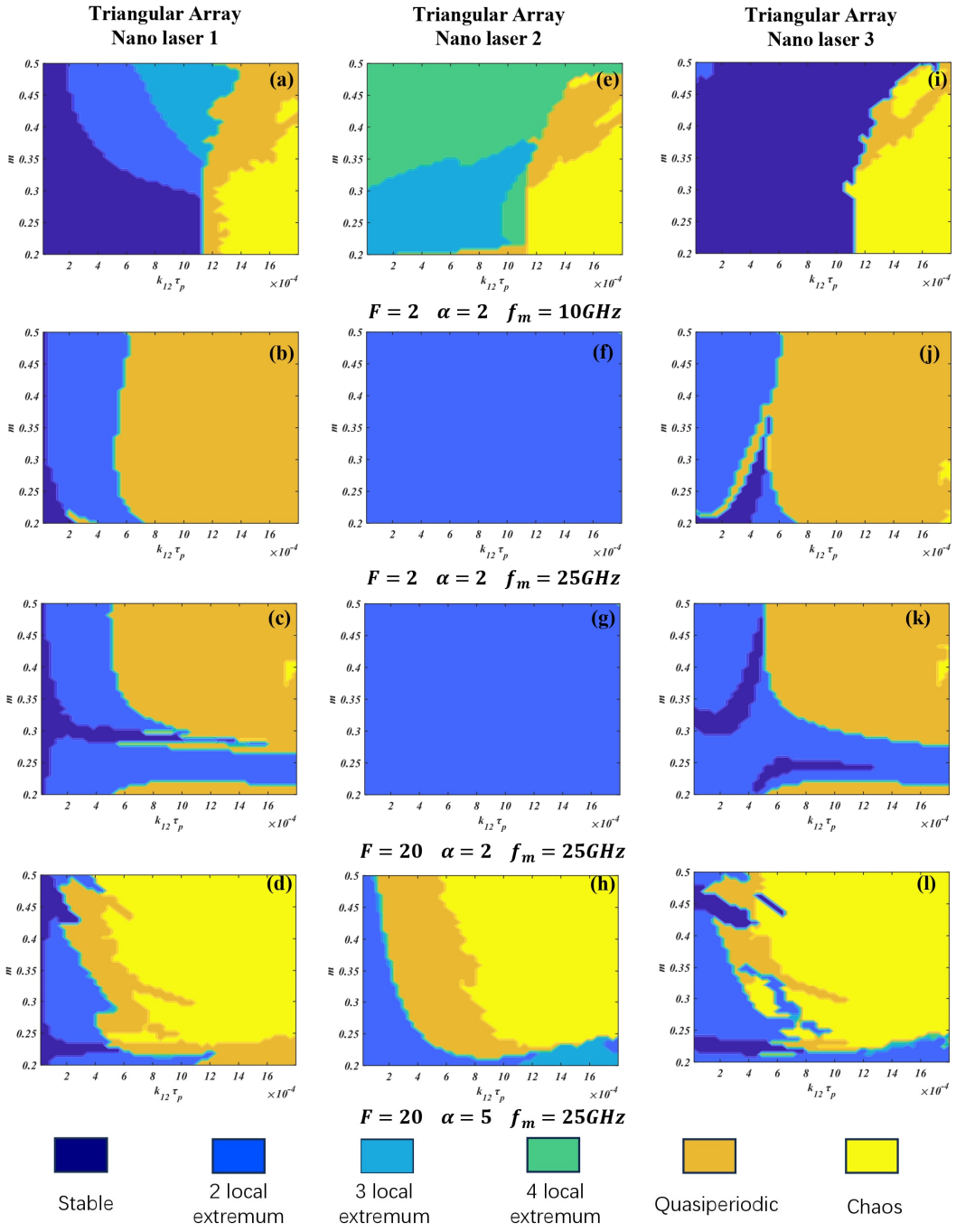

Figure 8. Two-dimensional maps of dynamics of 3-element triangular-array nano-lasers 1–3 with modulation for different F, different α, and different f_m values when $k_{23}\tau_p = 1.8 \times 10^{-4}$ and $I_0 = 2\,I$th.

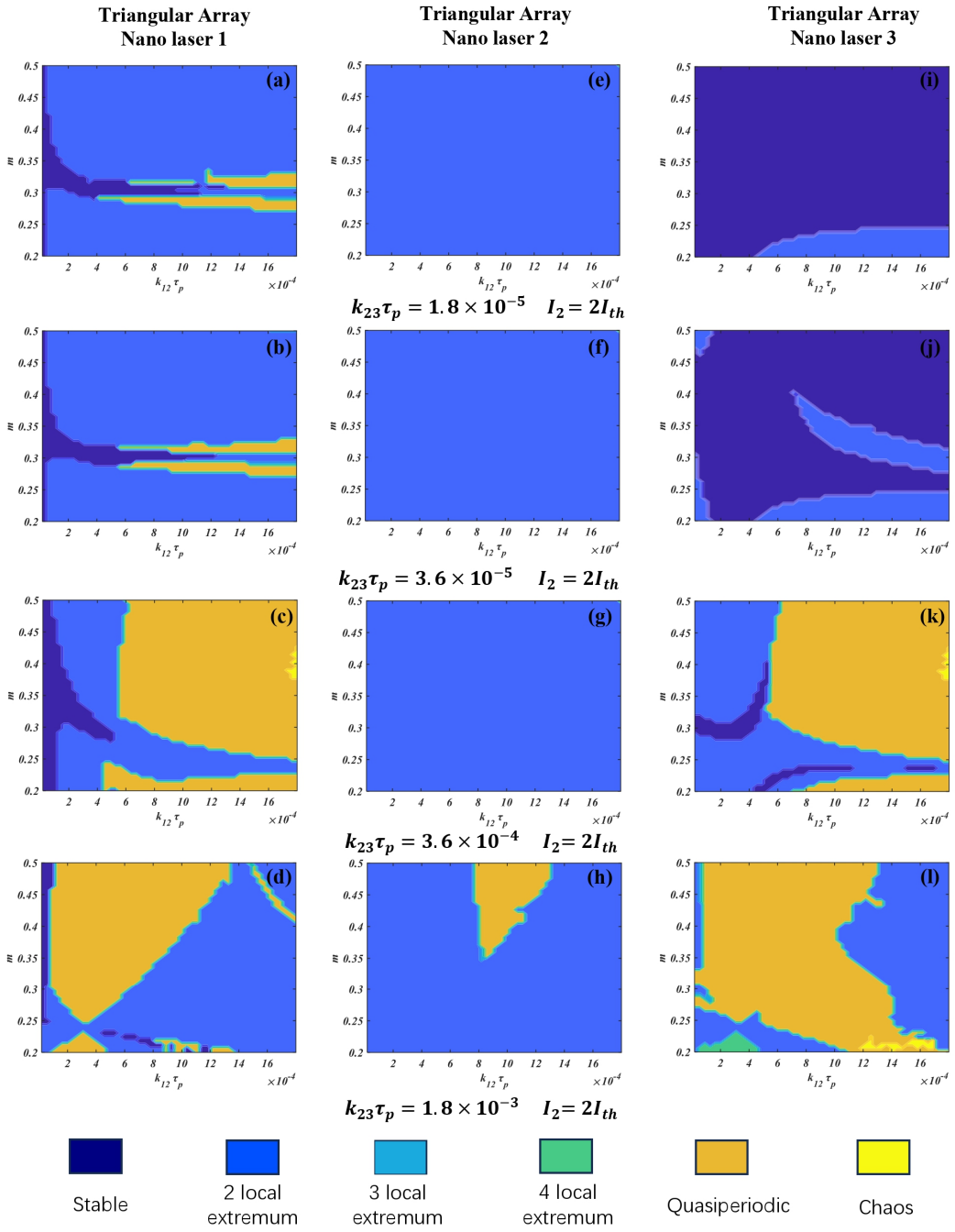

Figure 9. Two-dimensional maps of dynamics of 3-element triangular-array nano-lasers 1–3 with modulation for different $k_{23}\tau_p$ values when $F = 20$, $\alpha = 2$, $f_m = 25$ GHz, and $I_0 = 2$ *I*th.

The behaviour of triangular arrays as the bias current is varied is displayed in Figure 10. Qualitatively, the impact of bias current variation is similar to that in linear arrays, albeit with different detailed structures. Thus, for nano-laser 1 (Figure 10a–c), lower bias currents offer an admixture of regular and irregular dynamics, but as the bias current is increased, the extent of a stable behaviour is drastically reduced. Nano-laser 2 (Figure 10d–f) offers a plethora of dynamic species at lower bias currents, but irregular dynamics are atrophied and then eliminated as the bias current is increased. For nano-laser 3 (Figure 10g–i), a lower bias current leads to significant domains of stable behaviour which are reduced and then eradicated as the bias current is increased. However, this case quasi-periodic behaviour persists as a strong feature at higher bias currents.

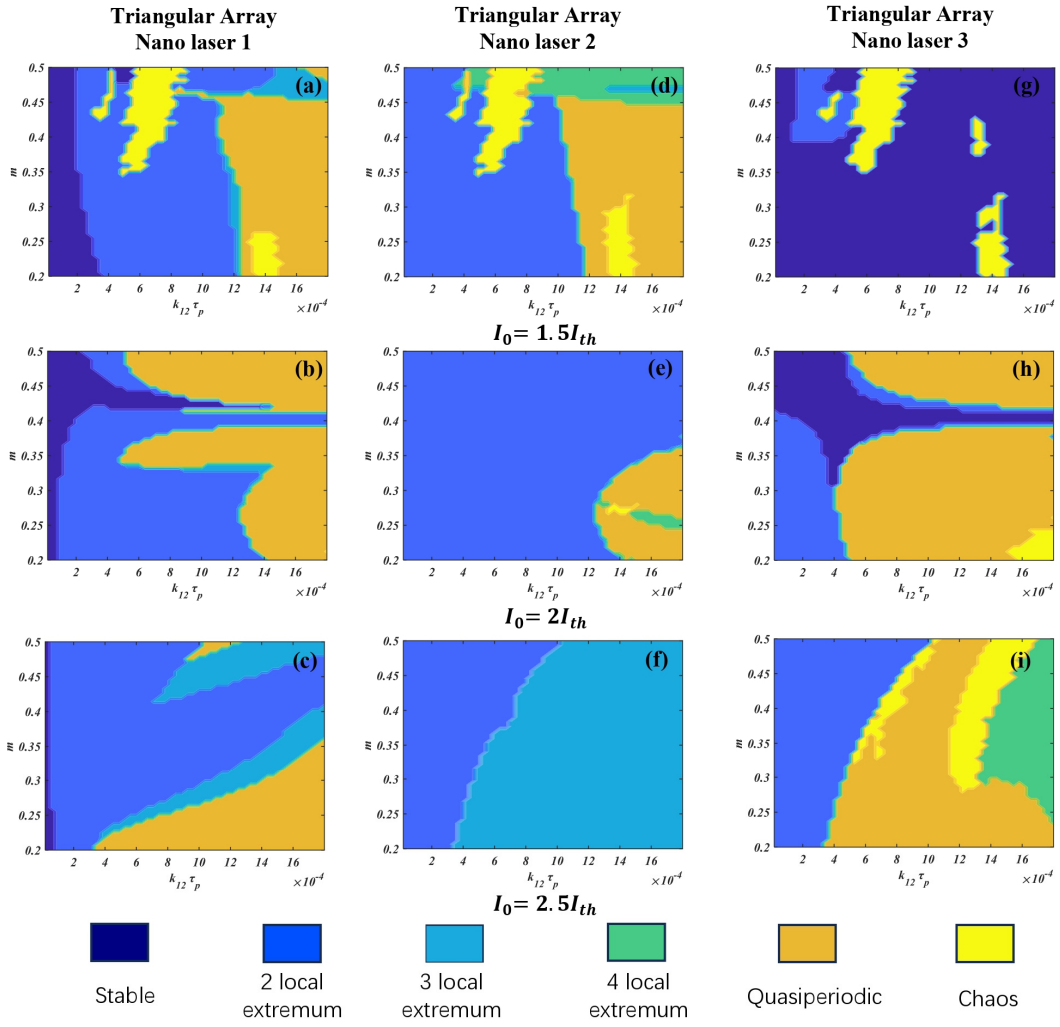

Figure 10. Two-dimensional maps of dynamics of 3-element triangular-array nano-lasers 1–3 with modulation for different I_0 values when $F = 40$, $\alpha = 2$, $f_m = 25$ GHz, and $k_{23}\tau_p = 1.8 \times 10^{-4}$.

The final set of results presented in Figure 11 explore the effects of varying the coupling strength between the lasers on the 2D maps described by the frequency detuning. Qualitatively, the impact of coupling strength variation is similar to that in linear arrays, albeit with different detailed structures. It is noted that, in both linear and triangular arrays, the stable region can be obtained by tuning the frequency between lasers even for a relatively large coupling strength.

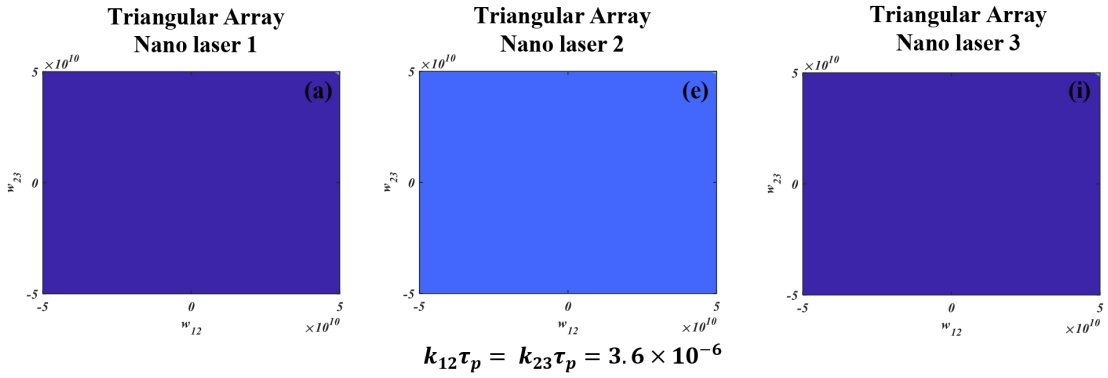

Figure 11. *Cont.*

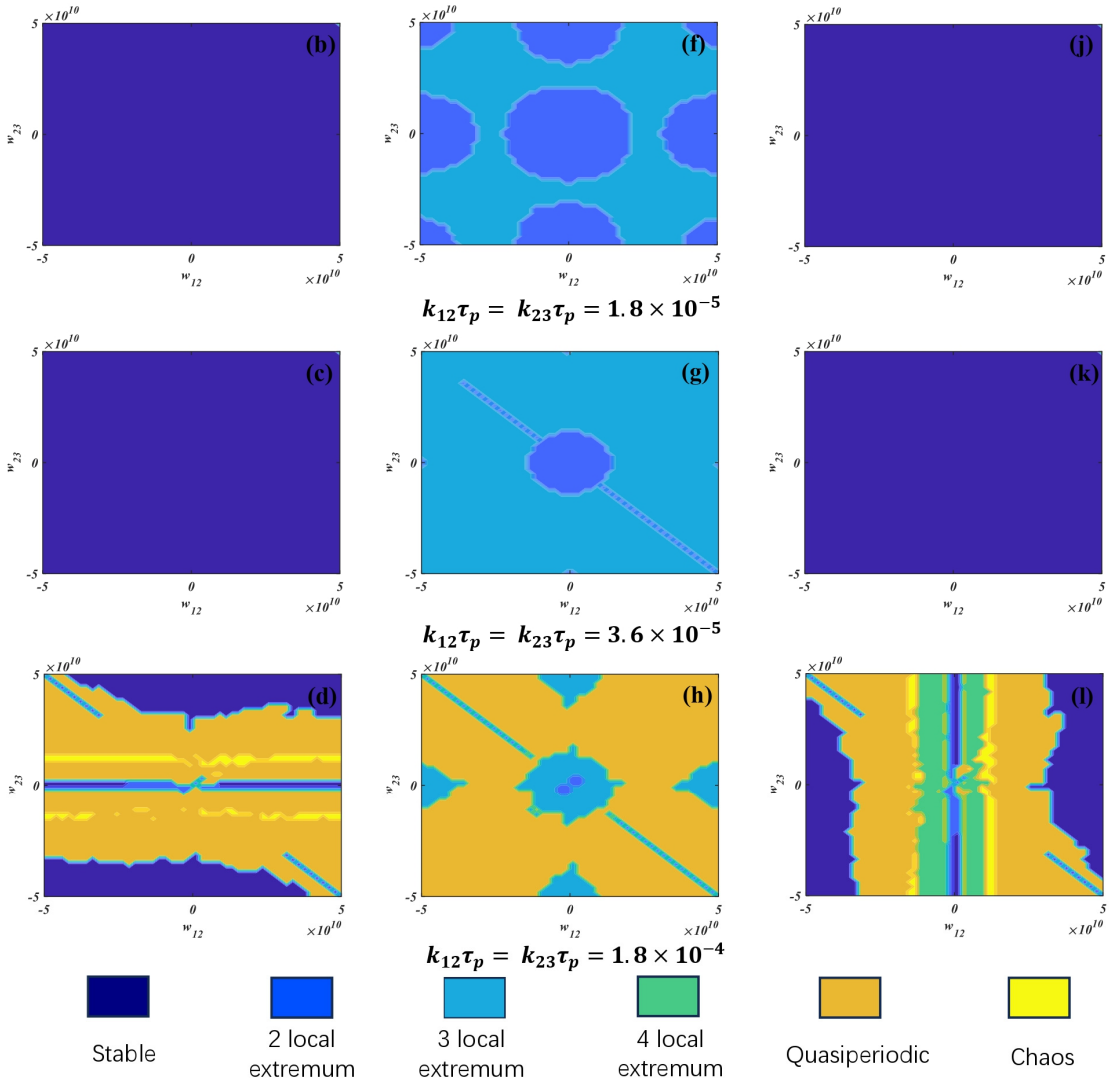

Figure 11. Two-dimensional maps of dynamics of 3-element triangular-array nano-lasers 1–3 with modulation for different $k_{13}\tau_p$ and $k_{23}\tau_p$ values when $F = 20$, $\alpha = 2$, $f_m = 25$ GHz, and $I_0 = 2$ Ith.

4. Conclusions

The salient feature of the present examination of the direct current modulation response of three-element nano-laser arrays is that these relatively simple configurations provide ready access to many forms of modulation response. Numerical simulations undertaken in this work show that both linear and triangular modulated nano-laser arrays can give rise to a wide variety of dynamics. In both cases, the interaction of the nano-lasers can range from zero-cross-talk to a complicated non-linear response. The actual response of the laser is significantly affected by modulation depth, modulation frequency, modulation bias current, frequency detuning, coupling strength, the linewidth enhancement factor, and the Purcell factor. We found that at a relatively low modulation frequency, the modulated nano-laser arrays with a low linewidth enhancement factor and Purcell factor have an extensive region of zero-cross-talk. In this region, the nano-lasers in the array act independently of each other. As has already been signalled, due to the several opportunities for affecting the direct current modulation response of these arrays, no claim is made of a definitive exploration of the species of their modulation response. A consideration of the response when more than one nano-laser is subject to direct current is expected to be of interest. The dynamic response of nano-laser arrays to other external stimuli will be examined in a future work.

Author Contributions: Conceptualization, K.A.S.; methodology, Y.F. and K.A.S.; software, Y.F. and S.A.; validation, Y.F., S.A. and K.A.S.; formal analysis, Y.F. and K.A.S.; investigation, Y.F. and K.A.S.; resources, X.S.; data curation, Y.F. and S.A.; writing—original draft preparation, Y.F. and K.A.S.; writing—review and editing, Y.F., K.A.S. and X.S.; visualization, Y.F. and S.A.; supervision, K.A.S. and X.S.; project administration, Y.F. and X.S.; funding acquisition, Y.F. and X.S. All authors have read and agreed to the published version of the manuscript.

Funding: This research was funded by the Proof of Concept Foundation of Xidian University Hangzhou Institute of Technology under Grant No. GNYZ2023QC0402.

Data Availability Statement: Data underlying the results presented in this paper are not publicly available at this time but may be obtained from the authors upon reasonable request.

Conflicts of Interest: The authors declare no conflict of interest.

References

1. Ning, C.Z. Semiconductor Nanolasers. *Phys. Status Solidi* **2010**, *247*, 774–788. [CrossRef]
2. Saxena, D.; Mokkapati, S.; Jagadish, C. Semiconductor Nanolasers. *IEEE Photonics J.* **2012**, *4*, 582–585. [CrossRef]
3. Gu, Q.; Fainman, Y. *Semiconductor Nanolasers*; Cambridge University Press: Cambridge, UK, 2017.
4. Ma, R.-M.; Oulton, R.F. Applications of Nanolasers. *Nat. Nanotechnol.* **2019**, *14*, 12–22. [CrossRef] [PubMed]
5. Nezhad, M.P.; Simic, A.; Bondarenko, O.; Slutsky, B.; Mizrahi, A.; Feng, L.; Lomakin, V.; Fainman, Y. Room-Temperature Subwavelength Metallo-Dielectric Lasers. *Nat. Nanotechnol.* **2010**, *4*, 395–399. [CrossRef]
6. Hou, Y.; Renwick, P.; Liu, B.; Bai, J.; Wang, T. Room Temperature Plasmonic Lasing in a Continuous Wave Operation Mode from an InGaN/GaN Single Nanorod with a Low Threshold. *Sci. Rep.* **2014**, *4*, 5014. [CrossRef]
7. Li, C.; Wright, J.B.; Liu, S.; Lu, P.; Figiel, J.J.; Leung, B.; Chow, W.W.; Brener, I.; Koleske, D.D.; Luk, T.-S.; et al. Nonpolar InGaN/GaN Core–Shell Single Nanowire Lasers. *Nano Lett.* **2017**, *17*, 1049–1055. [CrossRef] [PubMed]
8. Song, D.I.; Yu, A.; Samutpraphoot, P.; Lee, J.; Kim, M.; Park, B.J.; Sipahigil, A.; Kim, M.-K. Three-Dimensional Programming of Nanolaser Arrays through a Single Optical Microfiber. *Optica* **2022**, *9*, 1424. [CrossRef]
9. Hill, M.T.; Oei, Y.-S.; Smalbrugge, B.; Zhu, Y.; De Vries, T.; Van Veldhoven, P.J.; Van Otten, F.W.M.; Eijkemans, T.J.; Turkiewicz, J.P.; De Waardt, H.; et al. Lasing in Metallic-Coated Nanocavities. *Nat. Photonics* **2007**, *1*, 589–594. [CrossRef]
10. Lee, J.H.; Khajavikhan, M.; Simic, A.; Gu, Q.; Bondarenko, O.; Slutsky, B.; Nezhad, M.P.; Fainman, Y. Electrically Pumped Sub-Wavelength Metallo-Dielectric Pedestal Pillar Lasers. *Opt. Express* **2011**, *19*, 21524. [CrossRef]
11. Ding, K.; Liu, Z.C.; Yin, L.J.; Hill, M.T.; Marell, M.J.H.; Van Veldhoven, P.J.; Nöetzel, R.; Ning, C.Z. Room-Temperature Continuous Wave Lasing in Deep-Subwavelength Metallic Cavities under Electrical Injection. *Phys. Rev. B* **2012**, *85*, 041301. [CrossRef]
12. Ding, K.; Hill, M.T.; Liu, Z.C.; Yin, L.J.; Van Veldhoven, P.J.; Ning, C.Z. Record Performance of Electrical Injection Sub-Wavelength Metallic-Cavity Semiconductor Lasers at Room Temperature. *Opt. Express* **2013**, *21*, 4728. [CrossRef]
13. Li, K.H.; Liu, X.; Wang, Q.; Zhao, S.; Mi, Z. Ultralow-Threshold Electrically Injected AlGaN Nanowire Ultraviolet Lasers on Si Operating at Low Temperature. *Nat. Nanotechnol.* **2015**, *10*, 140–144. [CrossRef]
14. Ren, K.; Li, C.; Fang, Z.; Feng, F. Recent Developments of Electrically Pumped Nanolasers. *Laser Photonics Rev.* **2023**, *17*, 2200758. [CrossRef]
15. Lorke, M.; Suhr, T.; Gregersen, N.; Mørk, J. Theory of Nanolaser Devices: Rate Equation Analysis versus Microscopic Theory. *Phys. Rev. B* **2013**, *87*, 205310. [CrossRef]
16. Romeira, B.; Fiore, A. Purcell Effect in the Stimulated and Spontaneous Emission Rates of Nanoscale Semiconductor Lasers. *IEEE J. Quantum Electron.* **2018**, *54*, 1–12. [CrossRef]
17. Fan, Y.; Hong, Y.; Li, P. Numerical Investigation on Feedback Insensitivity in Semiconductor Nanolasers. *IEEE J. Sel. Top. Quantum Electron.* **2019**, *25*. [CrossRef]
18. Sattar, Z.; Shore, K. Analysis of the Direct Modulation Response of Nanowire Lasers. *J. Light. Technol.* **2015**, *33*, 3028–3033. [CrossRef]
19. Jiang, P.; Zhou, P.; Li, N.; Mu, P.; Li, X. Optically Injected Nanolasers for Time-Delay Signature Suppression and Communications. *Opt. Express* **2020**, *28*, 26421. [CrossRef] [PubMed]
20. Rasmussen, T.S.; Mork, J. Theory of Microscopic Semiconductor Lasers with External Optical Feedback. *Opt. Express* **2021**, *29*, 14182. [CrossRef] [PubMed]
21. Abdul Sattar, Z.; Shore, K.A. Phase Conjugate Feedback Effects in Nano-Lasers. *IEEE J. Quantum Electron.* **2016**, *52*. [CrossRef]
22. Han, H.; Shore, K.A. Dynamics and Stability of Mutually Coupled Nano-Lasers. *IEEE J. Quantum Electron.* **2016**, *52*, 1–6. [CrossRef]
23. Deka, S.S.; Jiang, S.; Pan, S.H.; Fainman, Y. Nanolaser Arrays: Toward Application-Driven Dense Integration. *Nanophotonics* **2020**, *10*, 149–169. [CrossRef]
24. Fan, Y.; Shore, K.A.; Shao, X. Dynamics of electrically-pumped semicondcutor nano-laser arrays. *Photonics* **2023**, *10*, 1249. [CrossRef]
25. Wang, S.S.; Winful, H.G. Dynamics of Phase-Locked Semiconductor Laser Arrays. *Appl. Phys. Lett.* **1988**, *52*, 1774–1776. [CrossRef]

26. Jiang, S.; Deka, S.; Pan, S.H.; Fainman, Y. Effects of High β on Phase-Locking Stability and Tunability in Laterally Coupled Lasers. *IEEE J. Sel. Top. Quantum Electron.* **2022**, *28*, 1–12. [CrossRef]
27. Suhr, T.; Gregersen, N.; Yvind, K.; Mørk, J. Modulation Response of NanoLEDs and Nanolasers Exploiting Purcell Enhanced Spontaneous Emission. *Opt. Express* **2010**, *18*, 11230. [CrossRef]
28. Coldren, L.A.; Corzine, S.W. *Diode Lasers and Photonic Integrated Circuits*; Wiley: New York, NY, USA, 1995.
29. Hong, H.; Shore, K.A. Modulated mutually coupled nanolasers. *IEEE J. Quantum Electron.* **2017**, *53*, 2000208.